

# Tuning the Polarizability in Donor Polymers with a Thiophenesaccharin Unit for Organic Photovoltaic Applications

Tao Xu, Luyao Lu, Tianyue Zheng, Jodi M. Szarko, Alexander Schneider,  
Lin X. Chen,\* and Luping Yu\*

This paper describes the synthesis of low bandgap copolymers incorporating an artificial sweetener derivative, *N*-alkyl, 3-oxothieno[3,4-*d*]isothiazole 1,1-dioxide (TID). This new TID unit is identical to the well-known thieno[3,4-*c*]pyrrole-4,6-dione (TPD) unit except that one carbonyl has been replaced by a sulfonyl group. Semi-empirical calculations on the local dipole moment change between ground and excited states ( $\Delta\mu_{ge}$ ) in the repeating units of the new polymer indicate that the replacement of the carbonyl by a sulfonyl group leads to larger  $\Delta\mu_{ge}$  values. The resulting polymers exhibit a diminished power-conversion efficiency (PCE) compared to a bulk heterojunction (BHJ) solar cells with PC<sub>71</sub>BM as an acceptor, which extends the correlation between PCE and  $\Delta\mu_{ge}$  of single repeating units in p-type polymers to a new regime. Detailed studies show that the strongly electron-withdrawing sulfonyl group is detrimental to charge separation in alternating copolymers containing a TID unit.

of the relationship between polymeric structure of the donor material and device performance. Among the factors that may influence solar energy conversion, the nature of electron donating and accepting materials and the morphology of the composites play the crucial roles in determining the final performance of the devices. In recent years, fullerene derivatives such as [6,6]-phenyl C<sub>71</sub>-butyric acid methyl ester (PC<sub>71</sub>BM) have been widely adopted as electron acceptors due to their low lying energy levels and relatively high electron affinity and mobility. It was also found that addition of a small amount of high boiling point solvent, generally 1,8-diiodooctane (DIO), can reliably improve the morphology of most of the composite systems.<sup>[19,20]</sup> Thus, we focus

## 1. Introduction

Bulk hetero-junction organic solar cells are complex systems; a synergistic approach is needed to optimize their performance.<sup>[1–6]</sup> Significant progress has been made in this field with the development of new polymeric structures,<sup>[7–14]</sup> optimization of processing conditions<sup>[15–17]</sup> and innovation of new device architecture.<sup>[18]</sup> A key challenge of the development of organic photovoltaic devices is obtaining a predictive understanding

our main effort on understanding the structure/property correlation of electron donor materials in order to develop innovative strategies for achieving high performance solar cells.

Numerous factors can influence the optical and electrical properties of low bandgap polymers. Our previous research indicated that the calculated internal dipole moment change between the ground and excited states of a polymer's repeating units,  $\Delta\mu_{ge}$ , showed a linear correlation with solar cell performance when other factors, such as morphology and charge carrier mobility, are comparable.<sup>[21,22]</sup> Crucial questions to be answered are that what will happen when  $\Delta\mu_{ge}$  is further increased, and why such a phenomenological model works well in a certain range. In this paper, calculations of dipolar change based on the polymer repeating units led us to identify two polymer systems, both copolymers containing benzodithiophene (BDT). One is based on thieno[3,4-*c*]pyrrole-4,6-dione (TPD) and the other on 3-oxothieno[3,4-*d*]isothiazole 1,1-dioxide (TID). The TPD unit has recently been incorporated into various low band gap conjugated polymer systems.<sup>[23–25]</sup> Previously explored as an artificial sweetener, TID unit bears both a sulfonyl and a carbonyl group, and is more electron deficient than TPD. The calculation results showed that the repeating units of both polymers containing TPD and TID (PPB and PID, respectively) exhibit a larger  $\Delta\mu_{ge}$  than our previous champion polymer PTB7. Thus, two polymers, PPB and PID, were synthesized and characterized

Dr. T. Xu, L. Y. Lu, T. Y. Zheng, A. Schneider,  
Prof. L. P. Yu  
Department of Chemistry  
and The James Franck Institute  
The University of Chicago  
Chicago, Illinois 60637, USA  
E-mail: lupingyu@uchicago.edu  
Dr. J. M. Szarko, Prof. L. X. Chen  
Department of Chemistry  
Northwestern University  
Evanston, Illinois 60208, USA  
E-mail: lchen@anl.gov  
Prof. L. X. Chen  
Chemical Science and Engineering Division  
Argonne National Laboratory  
Lemont, Illinois 60439, USA



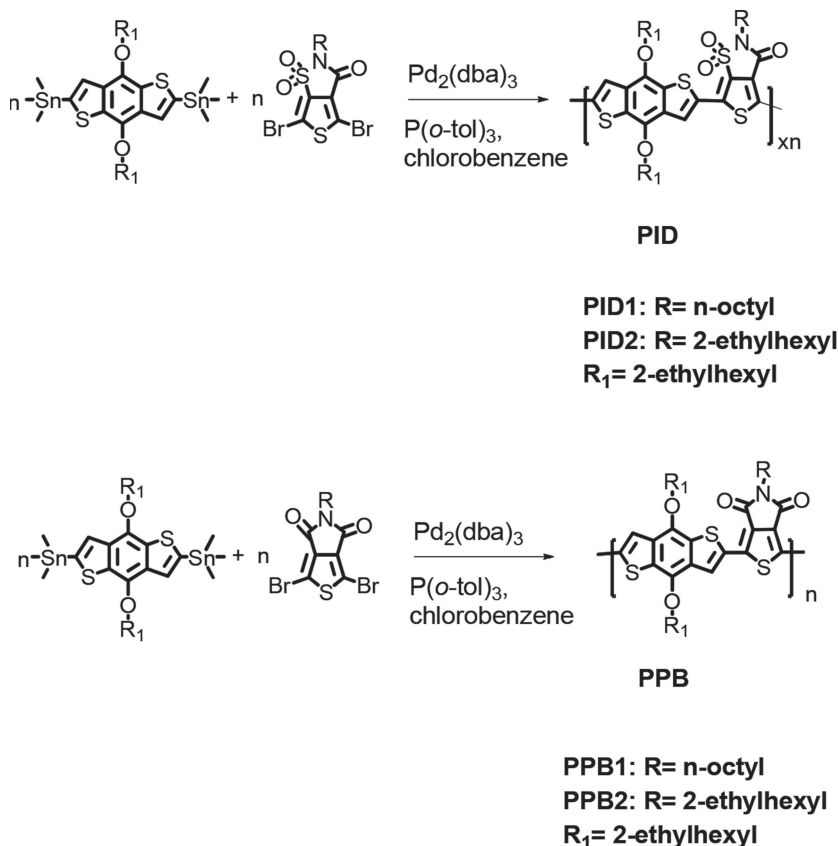
DOI: 10.1002/adfm.201303688

under identical conditions to investigate the effect of further increasing  $\Delta\mu_{\text{ge}}$  on solar cell performance. The results showed a clear decrease in device PCE as the  $\Delta\mu_{\text{ge}}$  increased further, indicating that an optimized  $\Delta\mu_{\text{ge}}$  value of around 4.0 Debye is needed to achieve a high PCE for organic photovoltaic (OPV) devices.

## 2. Results and Discussion

### 2.1. Synthesis of Polymers

The TID unit was prepared according to a modified literature procedure.<sup>[26]</sup> In order to anchor alkyl side chains on the original artificial sweetener unit, the phase transfer catalyst 15-crown-5 was used to achieve a relatively high conversion yield. Two different solubilizing alkyl side chains were used, octyl and 2-ethylhexyl (used in PID1 and 2, respectively). The final monomer TID was prepared via a modified bromination procedure in the presence of strong Brønsted acids (see Scheme S1 for synthetic details). The BDT and TPD units were synthesized according to previous published procedures.<sup>[7,27]</sup> Polymers were synthesized via Stille polycondensation using  $\text{Pd}_2(\text{dba})_3/\text{P}(\text{o-tolyl})_3$  catalyst in refluxing chlorobenzene (CB) for 48 h.<sup>[6,28]</sup> For comparison, another known polymer with a relatively large  $\Delta\mu_{\text{ge}}$  value (PPB) was also synthesized and characterized in the same conditions as Scheme 1.



**Scheme 1.** Synthetic routes to the polymers.

### 2.2. Optical and Electrical Properties of Polymers

As shown by gel permeation chromatography (GPC) measurements, these polymers exhibit number-averaged molecular weights between 12.0 and 18.6 kg/mol with a dispersity index ( $\bar{D}$ ) around 2 (Table S1). The structures of polymers were confirmed by  $^1\text{H}$  NMR spectra (Figure S1–S11) and elemental analyses (Table S2). Both the solution and thin-film optical absorption spectra of the polymers are presented in Figure 1. All polymers showed similar absorption range from 320 to 700 nm, and the absorption edge was nearly identical. The absorption maximum of the PID polymers was slightly blue-shifted compared to the PPB polymers. The cyclic voltammetry (CV) (Figure S12) studies indicated that the HOMO energy levels of PID1 and PID2 were at  $-5.44$  and  $-5.52$  eV, approximately 0.1 eV lower than their corresponding PPBs; while the LUMO energy levels were at  $-3.55$  eV and  $-3.50$  eV, respectively.

### 2.3. Current-Voltage ( $J$ – $V$ ) Characteristics of the Polymer Solar Cells

The photovoltaic properties were investigated in the device structure ITO/PEDOT:PSS/polymer:[6,6]-phenyl-C71-butyric acid methyl ester ( $\text{PC}_{71}\text{BM}$ )/Ca/Al. All solar cell data used in comparison of physical properties were determined based on this device structure. The active layers of  $\sim 100$  nm were spin-coated from 10 mg/mL chlorobenzene (CB) and DIO (v/v, 97:3) solutions. The corresponding  $J$ – $V$  curves of the four polymer solar cells under AM 1.5G condition at  $100 \text{ mW/cm}^2$  are presented in Figure 2a. Representative characteristics of solar cells are summarized in Table 1. Devices fabricated from PID1, PID2, PPB1 and PPB2 showed best PCE values at 3.28%, 3.05%, 5.97%, and 4.48%, respectively. Figure 2b depicts the external quantum efficiency (EQE) curves of the four solar cells. The PPB1 showed highest EQE values around 60% within the spectral range from 450 to 650 nm while PID2 showed the lowest EQE values ca 30%. Changes in EQE curves are in good agreement with the observed  $J_{\text{sc}}$  values from the four polymers. Hole mobility of all four polymers, measured using space charge limited current (SCLC)<sup>[29]</sup> method, were  $\sim 2.42 \times 10^{-4}$ ,  $2.71 \times 10^{-4}$ ,  $3.69 \times 10^{-4}$  and  $3.34 \times 10^{-4} \text{ cm}^2 \text{ V}^{-1} \text{ s}^{-1}$  for PID1, PID2, PPB1 and PPB2, respectively (Figure S13). Along with the EQE curves, the mobility values match with the  $J_{\text{sc}}$  trend well. Although PIDs exhibits high open circuit voltage due to a low HOMO energy level, small current density and low fill factor limit the overall solar cell performance.

To ensure that the comparison of solar cell performance is meaningful, the morphologies of these polymer films were optimized for the device performance by using organic additive in the film fabrication.<sup>[30]</sup> As shown

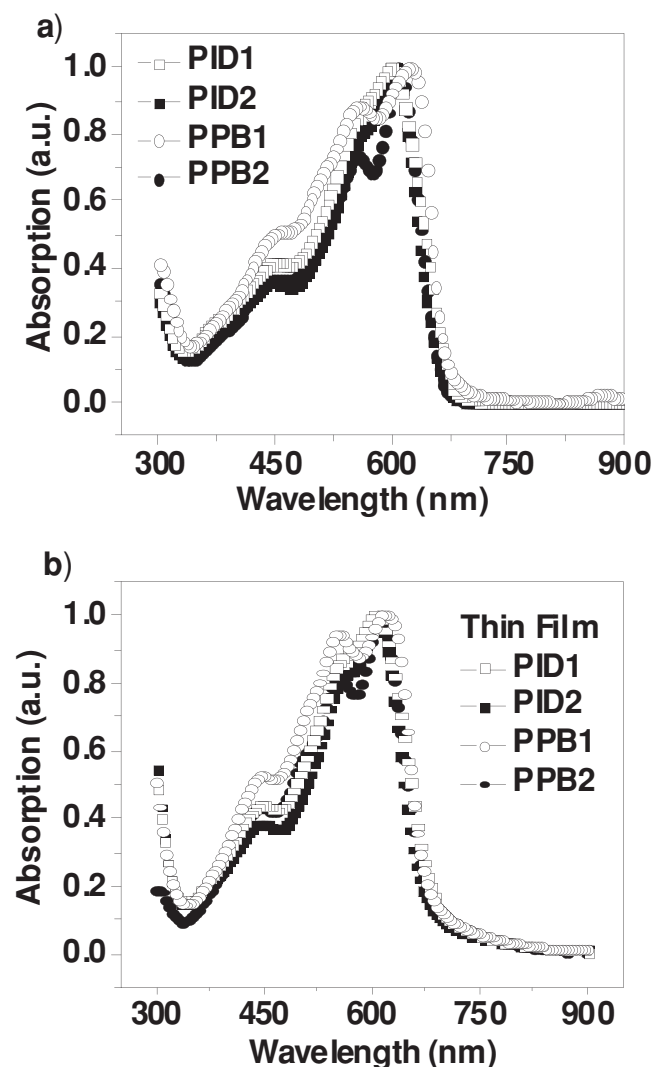


**Figure 1.** Normalized UV-vis absorption spectra of the polymers (a) in diluted chloroform solution and b) in pristine polymer films.

in the transmission electron microscopy (TEM) images of blend films with and without DIO in Figure S14, all four solar cells with DIO exhibit fine phase separations while severe phase segregation was observed in the blend films without DIO, leading to almost zero photovoltaic effect (Figure S15).

## 2.4. GIWAX Measurement

An interesting observation is that although the sulfonyl group adopts tetrahedron geometry with two oxygen atoms pointing out of the polymeric conjugation plane, the corresponding polymers exhibit enhanced backbone interactions, evidenced by the high crystallinity as clearly shown by GIWAXS results. The GIWAXS spectra showed a narrow peak width in the PID1 film, indicating a higher coherence length (3.5 nm) than that of the PPB1 (1.7 nm).<sup>[31]</sup> Accompanying this is a strong scattering peak (010) with a d-spacing of 3.4 Å for pure polymer thin film of PID1, (Figure S16), shorter than its corresponding

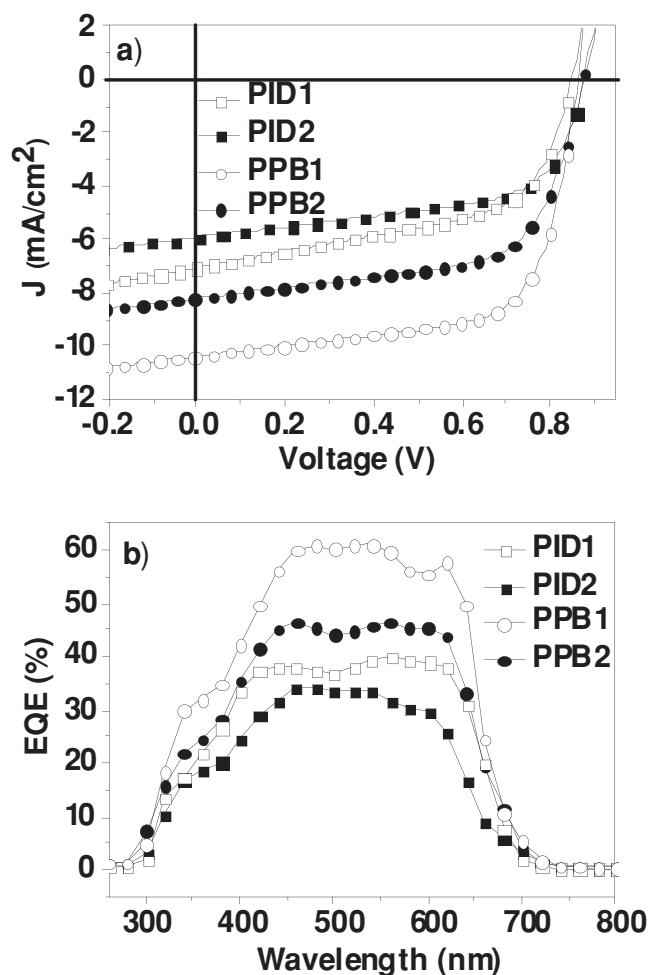


**Figure 2.** (a) Characteristic J-V curves of the four solar cells and (b) EQE curves of the four solar cells.

PPB1 polymer (Table S3). However, this strong interaction does not lead to higher mobility than PPB1, which is consistent with the possible role of trapping center to be discussed below.

Although the crystal structure studies are still preliminary, it can be assumed that the smaller  $\pi$ - $\pi$  stacking spacing is caused when the backbone is shifted parallel so that the tetrahedron sulfonyl groups can slip into each other. The  $\pi$ - $\pi$  stacking peaks are more prominent in the out-plane direction, which implies that the polymer chains tend to adopt a parallel orientation to the substrate. When it was blended with PC<sub>71</sub>BM in the absence of additive, the strong interaction still exists although the signal was weakened. Along with severe phase segregation observed in the TEM images, this explained why no photovoltaic effect was observed. After the addition of DIO to the composite, the  $\pi$ -packing is partially disrupted, however, the morphology is optimized by intercalation and the photovoltaic effect is enhanced.

## 2.5. Correlation of $\Delta\mu_{ge}$ Change and Solar Cell Performance

The results shown are those for the optimized solar cells and therefore it is believable to use them to compare with other

**Table 1.** Comparison of Photovoltaic Parameters of TID and TPD-containing Polymers in the Blend with PC<sub>71</sub>BM (CB/DIO, Polymer/PCBM = 1:1.5 weight ratio).

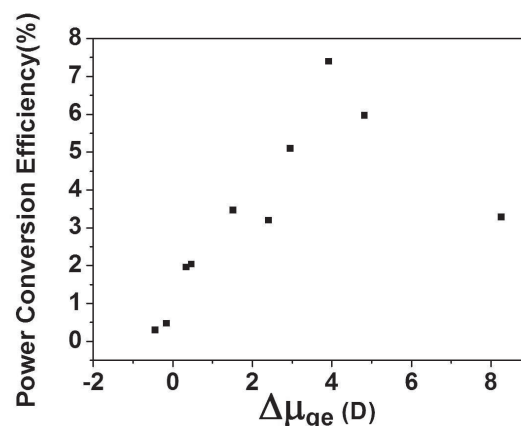
Polymer	HOMO* [eV]	LUMO* [eV]	V <sub>oc</sub> [V]	J <sub>sc</sub> [mA/cm <sup>2</sup> ]	FF [%]	PCE [%]
PID1	−5.44	−3.55	0.85	7.06	54.7	3.28
PID2	−5.52	−3.40	0.88	5.94	58.6	3.05
PPB1	−5.38	−3.55	0.86	10.40	66.6	5.97
PPB2	−5.40	−3.55	0.88	8.23	62.2	4.48

Note: \* From CV data.

similarly optimized systems. The dipole moments of single repeating units in PID1 and PPB1 were calculated using the procedure in our previous study.<sup>[18]</sup> The results are presented together with the optimized PCE values in **Table 2** along with data for other polymers previously reported. To simulate the randomized orientation of the asymmetric TID unit, the average dipole moment for each polymer repeating unit was determined and used for the analysis of dependence of PCE values on dipole changes. Both the ground and excited state dipole moments were calculated for each polymer repeating unit in the series. The overall change  $\Delta\mu_{ge}$  was calculated by accounting for the changes of the dipole along each coordinate axis. Our previous data indicated that a linear correlation between  $\Delta\mu_{ge}$  and PCEs exists, where the PTB7 showed the highest values of both PCE (7.4%) and  $\Delta\mu_{ge}$  (3.92 D). Such a trend was explained as an indication of local electron density gradient that defrays a part of the exciton binding energy, which enabled the cation generation in these polymers via intra-chain charge transfer even in solution.<sup>[32]</sup> However, the results shown here indicate that further increasing  $\Delta\mu_{ge}$  actually lowers PCE in the corresponding solar cell. PPB1 has a larger  $\Delta\mu_{ge}$ , but a lower PCE value of 5.97% than PTB7. The most notable dipole moment change  $\Delta\mu_{ge}$  comes from the TID-based polymer PID1 which is almost twice as large as PTB7. However, it exhibits a PCE value only slightly above 3%, indicating that the linear relationship of  $\Delta\mu_{ge}$  vs PCE did not extend (**Figure 3**) into the larger  $\Delta\mu_{ge}$  regime.

**Table 2.** Calculated Single Repeating Unit Dipole Moments and the Corresponding Optimized PCE Values.

Polymer	$\mu_g$ [D]	$\mu_e$ [D]	$\Delta\mu_{ge}$ [D]	PCE [%]
PTB2	3.60	6.37	2.96	5.10
PTB7	3.76	7.13	3.92	7.40
PTBF2	3.35	5.45	2.41	3.20
PBB3	0.61	0.82	0.47	2.04
PBIT1	4.46	4.80	0.34	1.96
PBIT3	6.99	6.83	−0.16	0.47
PBTZ1	0.88	2.41	1.52	3.46
PBTZ2	1.92	1.48	−0.44	0.29
PPB1	3.58	7.60	4.82	5.97
PID1	4.69	12.08	8.26	3.28

**Figure 3.** Correlation of PCE values with calculated dipolar changes of polymer repeating unit.

To explain these trends, we can reason that a higher  $\Delta\mu_{ge}$  implies a larger displacement of hole-electron pair in an exciton, lower Coulombic interactions between charges, and hence a reduced exciton binding energy. In addition, the introduction of strong electron withdrawing group simultaneously enhances the polarizability of excitons and lowers the polymer LUMO energy level. Ideally, the polarized exciton facilitates an electron transfer from the polymer blocks with lower electron affinity to the adjacent blocks with higher electron affinity and then to fullerene. However, the sulfonyl group exhibits strong electron accepting ability, leading to a much larger  $\Delta\mu_{ge}$  (8.26 D) than PTB7 (3.92 D) and a highly polarized exciton with a larger effective separation of charges within a polymer repeating unit and beyond. When  $\Delta\mu_{ge}$  is too large, the polarized polymer repeating units could also act as trapping or recombination centers for electrons and compete with the electron injection to the fullerene. This happens in the PPB and PID series of polymers, particularly PID1, with LUMO energy nearly 0.24 eV lower than that of PTB7. Ultrafast spectroscopic results, taken at 840 nm at which the cationic state absorption of the PID or PPB polymer in blended films dominates, confirmed this hypothesis. Although the rising time of the PID1 cation signal is still nearly 1 ps, the intramolecular charge separation (CS) dynamics in PID1 are slower than those of PTB7. The charge recombination (CR) of the cationic state, however, is relatively fast for the PID1 polymer. The CR traces of the PID1 polymer were fit to a tri-exponential decay of 2 ps, 60 ps, and >2 ns. At 3 ns, the cationic signal of only <10% remains, which is much smaller than those in PTB7 (**Figure 4**). The increased recombination rate is attributed to the increased binding energy of the bound charge transfer state within the polymer, which enhance the recombination probability. These results seem to indicate that the TID unit is too strong in electron-withdrawing ability to be useful in heteropolymers used as donor materials. An optimized polarizability in polymer repeating units is achieved with a  $\Delta\mu_{ge}$  around 4 Debye. Of course, we are aware of the complexity of the BHJ OPV system and only take this correlation as a useful guideline to design new materials. Detailed theoretical studies will certainly be needed to shed light in the validity of this relationship.

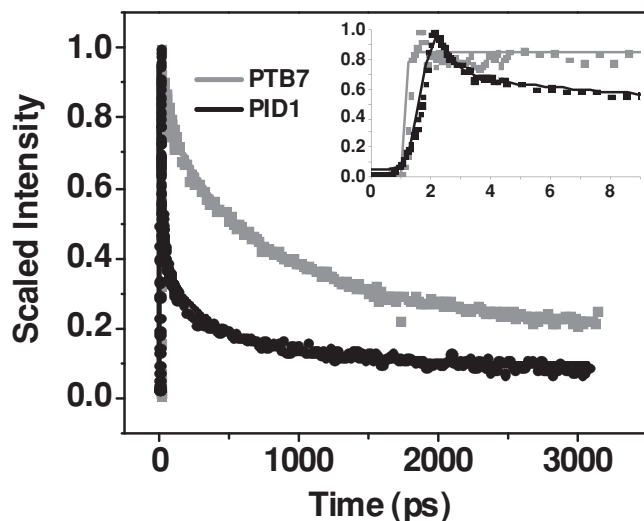


**Figure 4.** The charge separation (rise) and recombination (decay) dynamics monitored at the signals of the cationic state in the PID1 polymer. For comparison, the CS and CR of PTB7 are also shown.

### 3. Conclusion

Device and material studies on a low bandgap polymer PID with an extraordinarily large dipole moment change  $\Delta\mu_{ge}$  extends our previous picture of the effect of internal dipole moments on the photovoltaic properties of BHJ solar cells. The sulfonyl group in our new TID moiety not only resulted in a large  $\Delta\mu_{ge}$  in the repeating unit, but also lowered the HOMO/LUMO energy levels of the corresponding polymers. It is shown that the previously observed positive linear correlation between the parameter  $\Delta\mu_{ge}$  and PCE values might reverse as the  $\Delta\mu_{ge}$  further increases. One of the possible reasons is that the stronger electron withdrawing group could create electron trapping or recombination centers, which would diminish the solar cell performance. A general strategy is that in order to match with the fullerene acceptor, a donor polymer with a  $\Delta\mu_{ge}$  around 4 Debye is desirable.

### 4. Experimental Section

**Synthesis of PID1:** 2-Octyl-2,3-dibromo-3-oxothieno[3,4-*d*]isothiazole 1,1-Dioxide (223 mg, 0.49 mmol) was weighted into a 25 mL round bottom flask together with 2,6-bis(trimethyltin)-4,8-di(2-ethylhexyloxy) benzo[1,2-*b*:4,5-*b'*]dithiophene (374 mg, 0.49 mmol).  $Pd_2(dba)_3$  (9 mg) was used as the catalyst with  $P(o\text{-tolyl})_3$  (12 mg) as the ligand. The flask was vacuumized and purged with argon in three successive cycles. Then anhydrous CB was injected into the mixture via a syringe. The polymerization was performed at 120 °C for 48 h under argon protection. A blue mixture was obtained and suction filtered through Celite to get rid of any palladium particles. The raw product was precipitated out in methanol and went through Soxhlet extraction by acetone, hexane and chloroform. The final polymers were again precipitated out in methanol and dried in vacuum, yielding PID1 (328 mg, 89.8%).  $^1H$  NMR (500 MHz,  $CDCl_3$ )  $\delta$  8.60–9.00 (br, 1 H), 7.60–8.10 (br, 1 H), 4.10–4.55 (br, 4 H), 3.60–4.00 (br, 2 H), 0.90–2.20 (br, 45H). Calcd for  $C_{39}H_{53}NO_5S_4$ : C 62.95, H 7.18, S 17.24; found: C 63.62, H 7.56, S 17.48.

Both polymers were synthesized through the same procedure as PID1 with respective monomers. They were all precipitated in methanol,

collected by filtration followed by Soxhlet extraction using acetone, hexane, and finally chloroform.

**Device Fabrication:** The polymers and PC<sub>70</sub>BM were stirred at 80 °C for 12 h under N<sub>2</sub> atmosphere in chlorobenzene and 1,8-diodooctane (97:3,v/v). The polymer concentration was 10 mg/mL. ITO glass substrate was cleaned in water, acetone and isopropyl alcohol under sonication. After that, ITO glasses were exposed to ultraviolet ozone irradiation for 60 min. 30 nm of PEDOT:PSS was spin-coated at 6000 rpm for 1 min onto ITO glasses and dried at 80 °C for 30 min. Active layers were spin coated using the as-prepared solutions in a glove box. 20 nm Ca and 80 nm Al cathodes were thermal evaporated in a glove box at a chamber pressure of  $\sim 1.0 \times 10^{-6}$  torr. The area of the solar cell is 3.14 mm<sup>2</sup>.

**Characterization:** J–V characteristics of solar cells were measured under 1-sun, AM 1.5G irradiation (100 mW/cm<sup>2</sup>) from a solar simulator with a Xe lamp. The EQE measurement system was composed of a 250 W QTH lamp as the light source, a filter wheel, a chopper, a monochromator, a lock-in amplifier and a calibrated silicon photodetector. Optical properties were measured by using a Shimadzu UV-2401PC UV-Vis spectrophotometer. Electrochemical studies were carried out by using Cyclic voltammetry (CV) with Ag/AgCl as the reference electrode while the redox potential of ferrocene/ferrocenium ( $Fc/Fc^+$ ) was measured under the same conditions for calibration.

**GIWAXS Measurements:** GIWAXS measurements were performed at the 8ID-E beamline at the Advanced Photon Source (APS), Argonne National Laboratory using x-rays with a wavelength of  $\lambda = 1.6868$  Å and a beam size of  $\sim 50$   $\mu$ m. The samples for the measurements were prepared on PEDOT:PSS modified Si substrates under the same conditions as those used for fabrication of solar cell devices.

### Supporting Information

Supporting Information is available from the Wiley Online Library or from the author.

### Acknowledgements

T. Xu and L. Y. Lu contributed equally to this work. The authors are thankful for the support of the US National Science Foundation grant (NSF-SEP-1229089), Air Force office of Scientific Research (FA9550-12-1-0061), and NSF MRSEC program at the University of Chicago. This research is also partially supported by the ANSER Center, an Energy Frontier Research Center funded by the US Department of Energy, Office of Science, Office of Basic Energy Sciences, under Award Number DE-SC0001059.

Received: October 30, 2013

Revised: December 20, 2013

Published online: February 18, 2014

- [1] C. J. Brabec, S. Gowrisanker, J. J. M. Halls, D. Laird, S. J. Jia, S. P. Williams, *Adv. Mater.* **2010**, 22, 3839.
- [2] F. He, L. P. Yu, *J. Phys. Chem. Lett.* **2011**, 2, 3102.
- [3] H. J. Son, B. Carsten, I. H. Jung, L. P. Yu, *Energy Environ. Sci.* **2012**, 5, 8158.
- [4] H. J. Son, F. He, B. Carsten, L. P. Yu, *J. Mater. Chem.* **2011**, 21, 18934.
- [5] H. Hoppe, N. S. Sariciftci, *J. Mater. Res.* **2004**, 19, 1924.
- [6] B. Carsten, F. He, H. J. Son, T. Xu, L. P. Yu, *Chem. Rev.* **2011**, 111, 1493.
- [7] Y. Y. Liang, Y. Wu, D. Q. Feng, S. T. Tsai, H. J. Son, G. Li, L. P. Yu, *J. Am. Chem. Soc.* **2009**, 131, 56.



- [8] Y. Y. Liang, D. Q. Feng, Y. Wu, S. T. Tsai, G. Li, C. Ray, L. P. Yu, *J. Am. Chem. Soc.* **2009**, *131*, 7792.
- [9] T.-Y. Chu, J. Lu, S. Beaupre, Y. Zhang, J.-R. Pouliot, S. Wakim, J. Zhou, M. Leclerc, Z. Li, J. Ding, Y. Tao, *J. Am. Chem. Soc.* **2011**, *133*, 4250.
- [10] S. C. Price, A. C. Stuart, L. Yang, H. Zhou, W. You, *J. Am. Chem. Soc.* **2011**, *133*, 4625.
- [11] N. Blouin, A. Michaud, D. Gendron, S. Wakim, E. Blair, R. Neagu-Plesu, M. Belletete, G. Durocher, Y. Tao, M. Leclerc, *J. Am. Chem. Soc.* **2008**, *130*, 732.
- [12] Z. He, C. Zhong, X. Huang, W.-Y. Wong, H. Wu, L. Chen, S. Su, Y. Cao, *Adv. Mater.* **2011**, *23*, 4636.
- [13] W. Y. Wong, X. Z. Wang, Z. He, A. B. Djuricic, C. T. Yip, K. Y. Cheung, H. Wang, C. S. K. Mak, W. K. Chan, *Nat. Mater.* **2007**, *6*, 521.
- [14] W.-Y. Wong, C.-L. Ho, *Acc. Chem. Res.* **2010**, *43*, 1246.
- [15] G. Li, V. Shrotriya, J. S. Huang, Y. Yao, T. Moriarty, K. Emery, Y. Yang, *Nat. Mater.* **2005**, *4*, 864.
- [16] L. Y. Lu, Z. Q. Luo, T. Xu, L. P. Yu, *Nano Lett.* **2013**, *13*, 59.
- [17] L. Y. Lu, T. Xu, W. Chen, J. M. Lee, Z. Q. Luo, I. H. Jung, H. I. Park, S. O. Kim, L. P. Yu, *Nano Lett.* **2013**, *13*, 2365.
- [18] S. H. Park, A. Roy, S. Beaupre, S. Cho, N. Coates, J. S. Moon, D. Moses, M. Leclerc, K. Lee, A. J. Heeger, *Nat. Photonics* **2009**, *3*, 297.
- [19] J. Peet, J. Y. Kim, N. E. Coates, W. L. Ma, D. Moses, A. J. Heeger, G. C. Bazan, *Nat. Mater.* **2007**, *6*, 497.
- [20] J. K. Lee, W. L. Ma, C. J. Brabec, J. Yuen, J. S. Moon, J. Y. Kim, K. Lee, G. C. Bazan, A. J. Heeger, *J. Am. Chem. Soc.* **2008**, *130*, 3619.
- [21] B. Carsten, J. M. Szarko, H. J. Son, W. Wang, L. Y. Lu, F. He, B. S. Rolczynski, S. J. Lou, L. X. Chen, L. P. Yu, *J. Am. Chem. Soc.* **2011**, *133*, 20468.
- [22] B. Carsten, J. M. Szarko, L. Y. Lu, H. J. Son, F. He, Y. Y. Botros, L. X. Chen, L. P. Yu, *Macromolecules* **2012**, *45*, 6390.
- [23] Y. P. Zou, A. Najari, P. Berrouard, S. Beaupre, B. R. Aich, Y. Tao, M. Leclerc, *J. Am. Chem. Soc.* **2010**, *132*, 5330.
- [24] C. Piliago, T. W. Holcombe, J. D. Douglas, C. H. Woo, P. M. Beaujuge, J. M. J. Frechet, *J. Am. Chem. Soc.* **2010**, *132*, 7595.
- [25] E. T. Hoke, K. Vandewal, J. A. Bartelt, W. R. Mateker, J. D. Douglas, R. Noriega, K. R. Graham, J. M. J. Fréchet, A. Salleo, M. D. McGehee, *Adv. Energy Mater.* **2013**, *3*, 220.
- [26] P. A. Rossy, W. Hoffmann, N. Muller, *J. Org. Chem.* **1980**, *45*, 617.
- [27] H. J. Son, W. Wang, T. Xu, Y. Y. Liang, Y. E. Wu, G. Li, L. P. Yu, *J. Am. Chem. Soc.* **2011**, *133*, 1885.
- [28] Z. N. Bao, W. K. Chan, L. P. Yu, *J. Am. Chem. Soc.* **1995**, *117*, 12426.
- [29] C. Goh, R. J. Kline, M. D. McGehee, E. N. Kadnikova, J. M. J. Frechet, *Appl. Phys. Lett.* **2005**, *86*.
- [30] S. J. Lou, J. M. Szarko, T. Xu, L. P. Yu, T. J. Marks, L. X. Chen, *J. Am. Chem. Soc.* **2011**, *133*, 20661.
- [31] W. Chen, T. Xu, F. He, W. Wang, C. Wang, J. Strzalka, Y. Liu, J. G. Wen, D. J. Miller, J. H. Chen, K. L. Hong, L. P. Yu, S. B. Darling, *Nano Lett.* **2011**, *11*, 3707.
- [32] B. S. Rolczynski, J. M. Szarko, H. J. Son, Y. Y. Liang, L. P. Yu, L. X. Chen, *J. Am. Chem. Soc.* **2012**, *134*, 4142.